A Japanese Family With Autosomal Dominant Oculocutaneous Albinism Type 4

Ryoko Oki,[1] Kisaburo Yamada,[1] Satoko Nakano,[1] Kenichi Kimoto,[1] Ken Yamamoto,[2] Hiroyuki Kondo,[3] and Toshiaki Kubota[1]

[1]Department of Ophthalmology, Oita University Faculty of Medicine, Oita, Japan
[2]Department of Medical Biochemistry, Kurume University School of Medicine, Kurume, Japan
[3]Department of Ophthalmology, School of Medicine, University of Occupational and Environmental Health, Japan, Kitakyushu, Japan

Correspondence: Toshiaki Kubota, Department of Ophthalmology, Oita University Faculty of Medicine, 1-1 Idaigaoka, Hasama-machi, Yufu-shi, Oita 879-5593, Japan; tkubota@oita-u.ac.jp.

Submitted: August 25, 2016
Accepted: January 15, 2017

Citation: Oki R, Yamada K, Nakano S, et al. A Japanese family with autosomal dominant oculocutaneous albinism type 4. *Invest Ophthalmol Vis Sci*. 2017;58:1008–1016. DOI: 10.1167/iovs.16-20612

Purpose. We report the clinical characteristics of a Japanese family with autosomal dominant oculocutaneous albinism and a *SLC45A2* gene mutation.

Methods. A total of 16 members of a Japanese family with general hypopigmentation and foveal hypoplasia underwent detailed clinical examinations. We evaluated the severity of foveal hypoplasia using spectral-domain optical coherence tomography (SD-OCT) and graded it according to the criteria of Thomas et al. DNA was extracted from 17 family members and used for genome-wide single nucleotide polymorphism genotyping and linkage analysis. Mutational search was performed for the *SLC45A2* gene responsible for oculocutaneous albinism type 4 (OCA4).

Results. All 16 patients exhibited hypopigmentation of their hair and/or iris. They showed foveal hypoplasia, including 3 patients with grade 1 foveal hypoplasia, 7 with grade 2, and 6 with grade 3. No patient had grade 4 foveal hypoplasia. Optical coherence tomography showed macular ganglion cell complex thinning in the temporal area, and a slight reduction of visual field sensitivity in the centrotemporal area. A maximum multipoint parametric logarithm of the odds (LOD) score of approximately 2.00 to 3.56 was obtained on chromosome 5, spanning approximately 7.2 Mb between rs13187570 and rs395967 that included the *SLC45A2* gene. All affected members showed a novel heterozygous variant, c.208T>C (p.Y70H), in the *SLC45A2* gene, which supported a diagnosis of OCA4.

Conclusions. The present study reports a very rare family with autosomal dominant OCA4 whose diagnosis was confirmed by a mutational analysis. Most family members exhibited mild general hypopigmentation and low-grade foveal hypoplasia.

Keywords: albinism, foveal hypoplasia, autosomal dominant

Oculocutaneous albinism (OCA) describes a group of autosomal recessive disorders featuring hypopigmentation of the hair, skin, and eyes due to an abnormality in the production of melanin. Ocular signs that reflect the abnormal development of the visual system in albinism include reduced visual acuity, nystagmus, strabismus, poor stereopsis, and foveal hypoplasia.[1] In albinism, more fibers from the temporal retina project to the contralateral hemisphere than normal.[2–4] It can be detected by recording the visual evoked potentials (VEPs). The VEP recordings of patients with albinism show a contralateral predominance in response to monocular stimulation.[5,6]

Seven types of human OCA (OCA 1–7) have been defined, based on their causative genetic mutations: tyrosinase (*TYR*),[7] P protein,[8] tyrosinase-related protein 1 (*TYRP1*),[9] the solute carrier family 45, membrane 2 (*SLC45A2*),[10] OCA5 (mapped to the 4q24), OCA6 (*SLC24A5*), and OCA7 (*C10orf11*).[11] A survey of Japanese OCA patients revealed that OCA1 was the most frequent type (34%), while OCA4, which is rare in other countries, is the second most frequent type (27%).[12] The clinical phenotypes of OCA4 vary from complete depigmentation to partial depigmentation with brown hair and iris; some patients show improvement in their appearance during the first decade of life. It has been hypothesized that these phenotypic variations of OCA4 patients are dependent on mutations in the *SLC45A2* gene.[13,14] A dominant OCA mutant strain has been isolated in a few animal species.[15,16] Thus far, however, to our knowledge autosomal dominant albinism has not yet been described in humans.

We report a family with foveal hypoplasia and generalized hypopigmentation, features consistent with OCA. A mutation screening analysis of the affected members showed a likely pathogenic variant in the *SLC45A2* gene, confirming a diagnosis of OCA4. To the best of our knowledge, this is the first report on a family with autosomal dominant OCA in which the diagnosis was confirmed by a genetic analysis. We described the clinical characteristics of the dominant OCA family, including the findings from the structural and functional examinations of the fovea in the patients without remarkable nystagmus.

Patients and Methods

This study adhered to the tenets of the Declaration of Helsinki and was approved by the Ethics Committee of Oita University

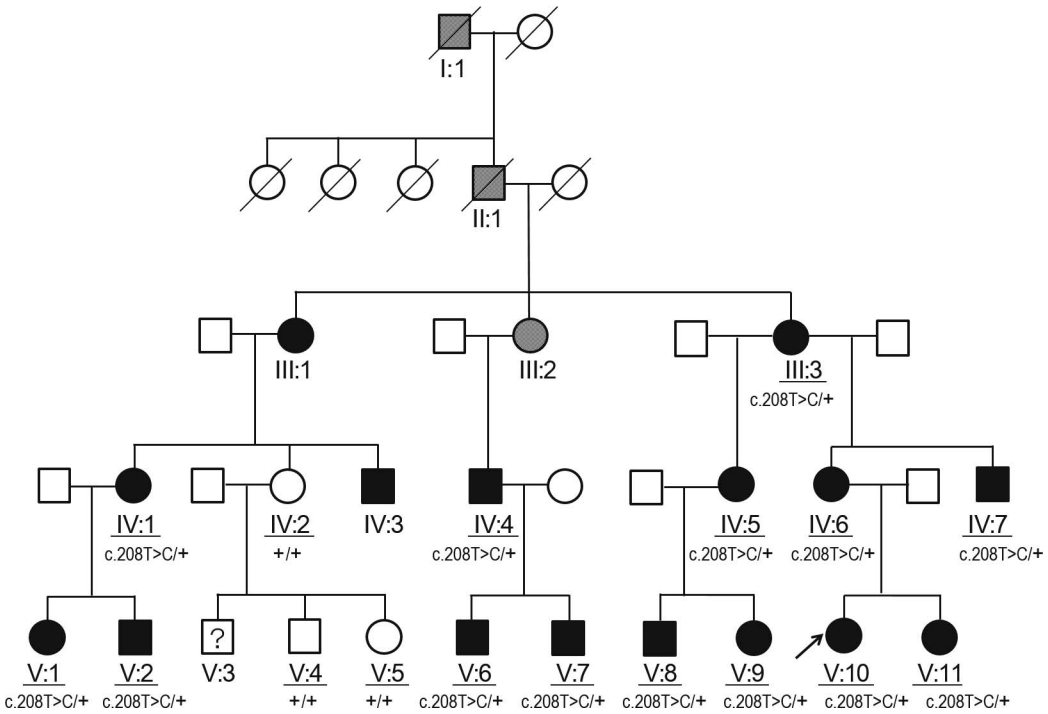

Figure 1. The pedigree of the Japanese family with autosomal dominant OCA4. The *SLC45A2* mutation (c.208T>C) was detected in all of the affected patients. The *black arrow* indicates the proband. The *black-filled symbols* indicate the patients who were affected by foveal hypoplasia. The *gray-filled symbols* indicate the patients in whom foveal hypoplasia was suspected due to poor vision, nystagmus, and hypopigmented hair. The *question marks* indicate the patients who did not undergo a clinical examination. The *underlined numbers* indicate the patients who underwent a molecular genetic analysis. The *plus signs* (+) show normal alleles.

Faculty of Medicine. Informed consent for the study was obtained from each patient. The proband was a 14-year-old female (V:10; Fig. 1) with amblyopia, congenital nystagmus, and hypopigmentation of the hair and iris. The family history revealed that many family members had amblyopia, nystagmus, and hypopigmented hair. The great-great-grandfather (I:1) and great-grandfather (II:1) of the proband exhibited similar features while they were alive. There was no history of consanguinity in this family. We examined 20 members in three generations of her family. Three members had normal foveal morphology (IV:2, V:4, V:5) and 16 had foveal hypoplasia (7 males, 9 females; age, 6–73 years). One member (III:2) showed foveal schisis; thus, we could not confirm the presence of hypoplasia. However, the patient was strongly suspected to have foveal hypoplasia due to the presence of amblyopia, nystagmus, and esotropia.

All 16 patients underwent a full ophthalmologic examination, which included assessments of decimal best corrected visual acuity (BCVA), refractive errors, type of nystagmus, ocular alignment and stereopsis, slit-lamp biomicroscopy, a fundus examination, and spectral-domain OCT (SD-OCT) imaging. Hypopigmentation of the irides, hair, and fundus was evaluated by a pediatric ophthalmology specialist (RO). Fundus photographs were taken using a digital fundus camera (VX-10; Kowa, Hamamatsu, Japan) to evaluate macular transparency according to a grading system previously described by Summers et al.[17] The grading of macular transparency was as follows: Grade 1, the choroidal vessels are easily visible in the macula; Grade 2, the choroidal vessels are visible in the macula but indistinct because of the translucent appearance of the retinal pigment epithelium; and Grade 3, the choroidal vessels are not visible in the macula because of the opaque quality of the pigment epithelium. Stereopsis was evaluated with a Titmus stereo test and a TNO stereo test. Nystagmus was determined by clinical observation and considered to be present even if it was latent or intermittent.

Spectral-domain OCT images of the subjects were acquired using a Spectralis OCT (Heidelberg Engineering, Heidelberg, Germany), which provides 40,000 A-scans per second with 7-μm optical and 3.5-μm digital axial resolution. Vertical line scans through the fovea were obtained for each patient. To minimize test errors caused by missing the fovea due to nystagmus or poor fixation, horizontal and vertical line scans through the fovea center were obtained at a 30° angle, followed by serial vertical scans with an examination field size of $30 \times 10°$. At each location of interest on the retina, 100 SD-OCT images were acquired and averaged to reduce speckle noise. Measurements were replicated by a skilled investigator (KY). We evaluated the severity of foveal hypoplasia from the OCT images. Foveal hypoplasia was graded according to the criteria of Thomas et al.[18] The grades were defined as follows: grade 1, a shallow foveal pit, presence of outer nuclear layer (ONL) widening, and presence of outer segment (OS) lengthening; grade 2, similar to grade 1 but with the absence of the foveal pit; grade 3, similar to grade 2 but with the absence of OS lengthening; grade 4, similar to grade 3 but with the absence of ONL widening.

Pattern VEPs were recorded in 3 patients (V:6, V:8, V:10) and a normal member (V:5) under the condition of monocular stimulation. The distribution of the potentials across the hemispheres was assessed by analyzing the amplitudes of the positive CI components,[6] which occurred at approximately 100 ms. Visual evoked potential asymmetry also was assessed by interocular polarity at the L-R trace, which indicates a difference in the potentials in the left and right hemispheres.

Four patients with foveal hypoplasia who had stable fixation, good visual acuity, and spherical refraction within

Table. The Clinical Characteristics of Japanese Patients From the Same Family With Autosomal Dominant OCA4

			BCVA		Refractive Error, D						Hypopigmentation		
Case No.	Sex	Age	R	L	R	L	Stereopsis	Strabismus	Nystagmus	Foveal Hypoplasia Grade	Hair	Iris	Macular Transparency Grade
IV:4	M	43	1.5	1.2	+0.75	+0.25	–	ET	–	1	–	+	3
V:2	M	14	1.2	1.5	+0.37	+0.50	240	X	+*	1	+	+	3
IV:1	F	48	0.9	1.0	−10.5	−7.75	1980	X	–	1	+	+	3
V:8	M	13	1.2	1.5	±0	−0.25	240	–	–	2	+	+	1
IV:7	M	37	1.0	1.2	−2.08	−4.13	–	ET	+*	2	+	+	3
V:1	F	17	1.0	1.0	−2.37	−2.38	400	X(T)	+*	2	+	+	3
V:6	M	14	0.8	1.0	−0.61	−0.25	480	–	–	2	–	+	3
IV:6	F	41	0.8	0.8	−8.50	−5.63	1980	–	+*	2	+	–	1
III:1	F	73	0.9	0.9	+3.75	+3.38	1980	X	+*	2	+	+	3
III:3	F	70	0.4	0.4	−2.88	−0.75	–	ET	+	2	+	+	1
V:11	F	8	0.7	0.7	−1.50	−2.75	800	X	+	3	+	–	1
V:10	F	14	0.6	0.7	−4.00	−2.88	–	–	+	3	+	–	2
V:9	F	7	0.5	0.3	+4.63	+4.88	–	X	+	3	–	+	3
IV:3	M	39	0.3	0.3	−2.75	−5.00	–	–	+	3	+	+	2
IV:5	F	44	0.3	0.3	−0.75	−1.13	–	ET	+	3	+	+	2
V:7	M	6	0.2	0.3	+2.75	+2.75	NE	–	+	3	+	+	3

* Nystagmus absent in the primary position. NE, not examined; +, present; –, not present; M, male; F, female; X, exophoria; X(T), intermittent exotropia; ET, esotropia; R, right; L, left.

±3.00 diopters (D) underwent additional examinations including the measurement of the ganglion cell complex (GCC) by OCT and a visual field examination. Macular GCC was evaluated with a 3D OCT-2000 (Topcon, Inc., Tokyo, Japan), using the 3D macular vertical scan protocols, which consist of a 7×7 mm^2 or 6×6 mm^2 analysis area containing 512 A scans/B scan with 128 B scans per volume. Ganglion cell complex thickness represents the distance from the internal limiting membrane to the outer boundary of the inner plexiform layer. The significance map is color-coded: yellow indicates border-

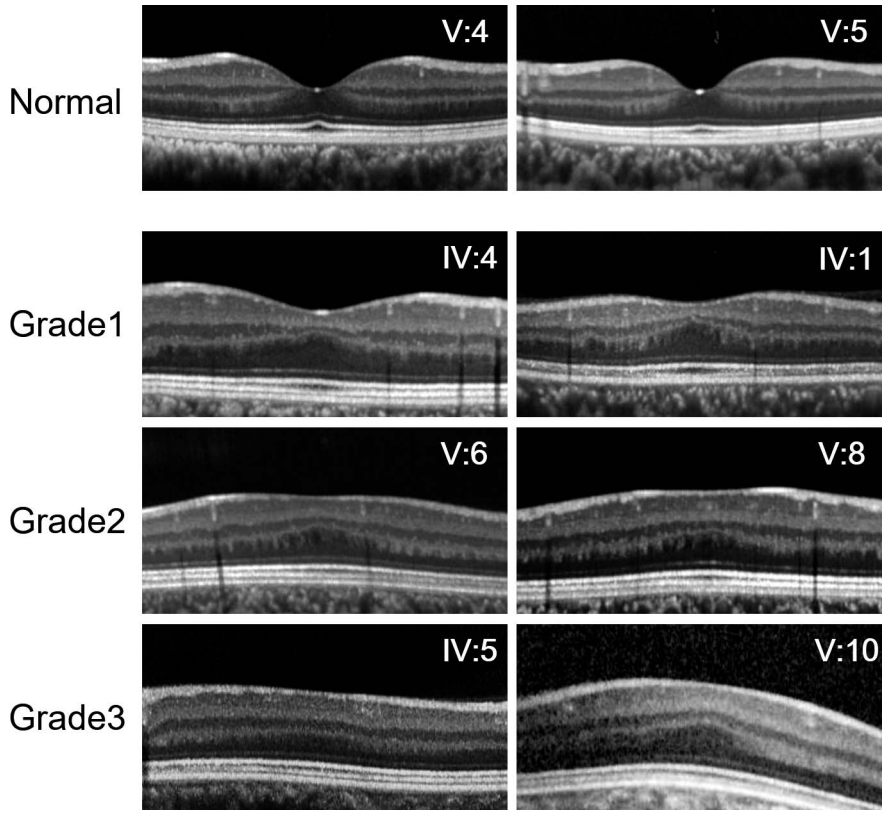

Figure 2. The structural grading of foveal hypoplasia by SD-OCT images from the affected members. Linear SD-OCT scans through the central macula in two unaffected members (V:4, V:5) and six patients (IV:1, IV:4, IV:5, V:6, V:8, and V:10). Grade 4 foveal hypoplasia was not observed in any of the family members.

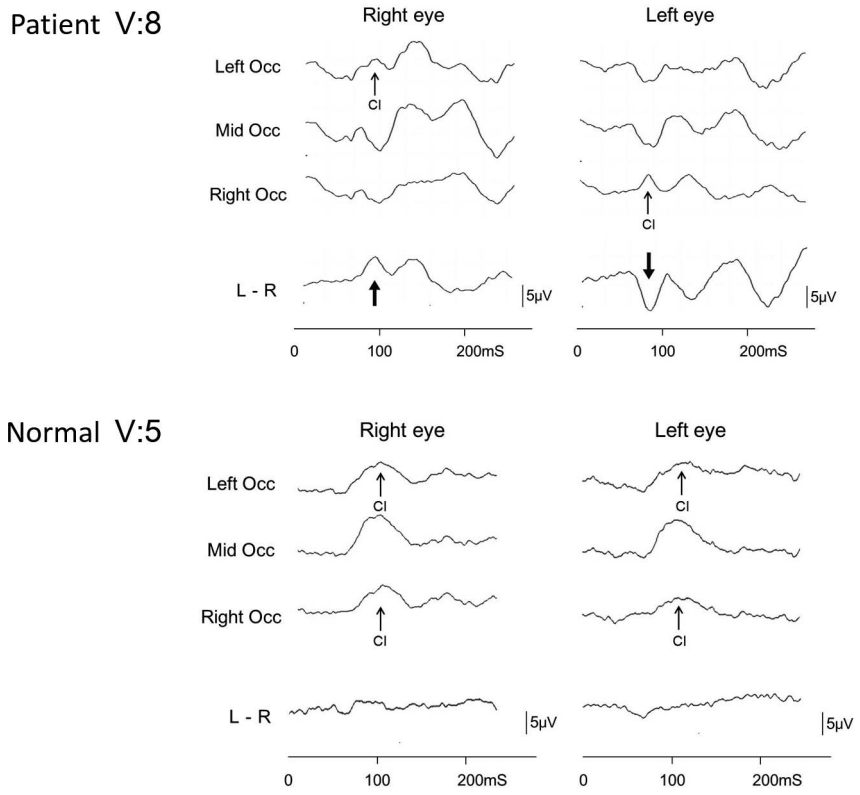

Figure 3. The pattern VEP of a patient (V:8) and a normal member (V:5). The pattern of the affected patient shows the CI component peaking across the left hemisphere while the left eye responses peak across the right hemisphere. Interocular inverse polarity (*arrow*, positive peak from the right eye and negative peak from the left eye), which was observed on the L-R trace, reflected the hemispheric asymmetry typically observed in albinism. In a normal individual, the pattern VEP shows no significant interhemispheric asymmetries.

line results ($P < 0.05$), and red represents results that are outside the normal limits ($P < 0.01$). A visual field examination was performed with a Humphrey Field Analyzer with the SITA 10-2 or 30-2 (Carl Zeiss Meditec, Inc., Jena, Germany).

Genomic DNA was extracted from leukocytes from peripheral blood samples. The Illumina HumanOmniExpress-24 v1.1 Array and the Illumina GenomeStudio v2011.1 single nucleotide polymorphism (SNP) genotyping system (Illumina, San Diego, CA, USA) were employed for genome-wide SNP typing according to the manufacturer's protocols. All SNP markers were tested for Mendelian error before linkage analysis so they could be excluded from further investigation. Multipoint parametric logarithm of the odds (LOD) scores were calculated using GeneHunter v2.1r5 (with easyLINKAGEPlus v5.08).[19,20] A total of 1748 and 68 SNPs whose pairwise r-square was 0.01 were automatically selected by easyLINKAGE for linkage analysis to the whole genome (2.0 cM spacing) and to 70 cM candidate region of chromosome 5 (1.0 cM spacing), respectively. The model used in the parametric analyses assumed a dominant model of inheritance, a disease allele frequency of 0.001 and complete penetrance. The marker genetic position was based on the Marshfield linkage map,[21] and the sex-averaged position was applied.

To screen mutations in the coding exons (exons 1–7) of the *SLC45A2* gene, oligonucleotide primers on the flanking intron and untranslated region sequences were designed (available on request). Polymerase chain reaction and Sanger sequencing were conducted for the affected proband (V:10) and an unaffected family member (IV:2). To investigate whether the c.208T>C change in the *SLC45A2* gene cosegregates with the disease, variation-specific PCR primers were designed: 5′-AAGAGAGTTCTGCTACGCGG-3′ and 5′-CCTGCTACAACAG TAGCCCC-3′. Polymerase chain reaction and direct Sanger sequencing were performed on 14 family members (Fig. 1). Sequences of the membrane–associated transporter protein (MATP), which is coded by the *SLC45A2* gene in humans and other vertebrates, were obtained from the University of California, Santa Cruz (UCSC; Santa Cruz, CA, USA) Genome Browser (available in the public domain at http://genome.cse.ucsc.edu/) and aligned against one another using the Clustal W software program, which is provided by the European Bioinformatics Institute (available in the public domain at http://www.ebi.ac.uk/). The pathogenicity of the amino acid changes was evaluated by four computational programs: Polyphen-2 (available in the public domain at http://genetics.bwh.harvard.edu/pph2/), SIFT (available in the public domain at http://sift.jcvi.org), PROVEAN (available in the public domain at http://provean.jcvi.org), and Mutation Taster (available in the public domain at http://www.mutationtaster.org).

Results

The clinical characteristics of OCA in these individuals are described in the Table. The spherical equivalent refractive error varied (−10.5 to +4.88 D). The binocular decimal BCVA ranged from 0.3 to 1.5 (median, 0.8). Seven patients had a decimal BCVA value of better than 1.0. Four patients had manifest esotropia; 6 had exophoria or intermittent exotropia. Of the 15 patients in whom stereo acuity was examined, 8 had poor stereopsis (240–1980 arc seconds) and 7 had no stereopsis. Four patients had no nystagmus, whereas 12 had horizontal nystagmus (5 of whom had nystagmus on lateral gaze but not in the primary position). Full ophthalmologic examinations and the OCT findings revealed that all 16 patients

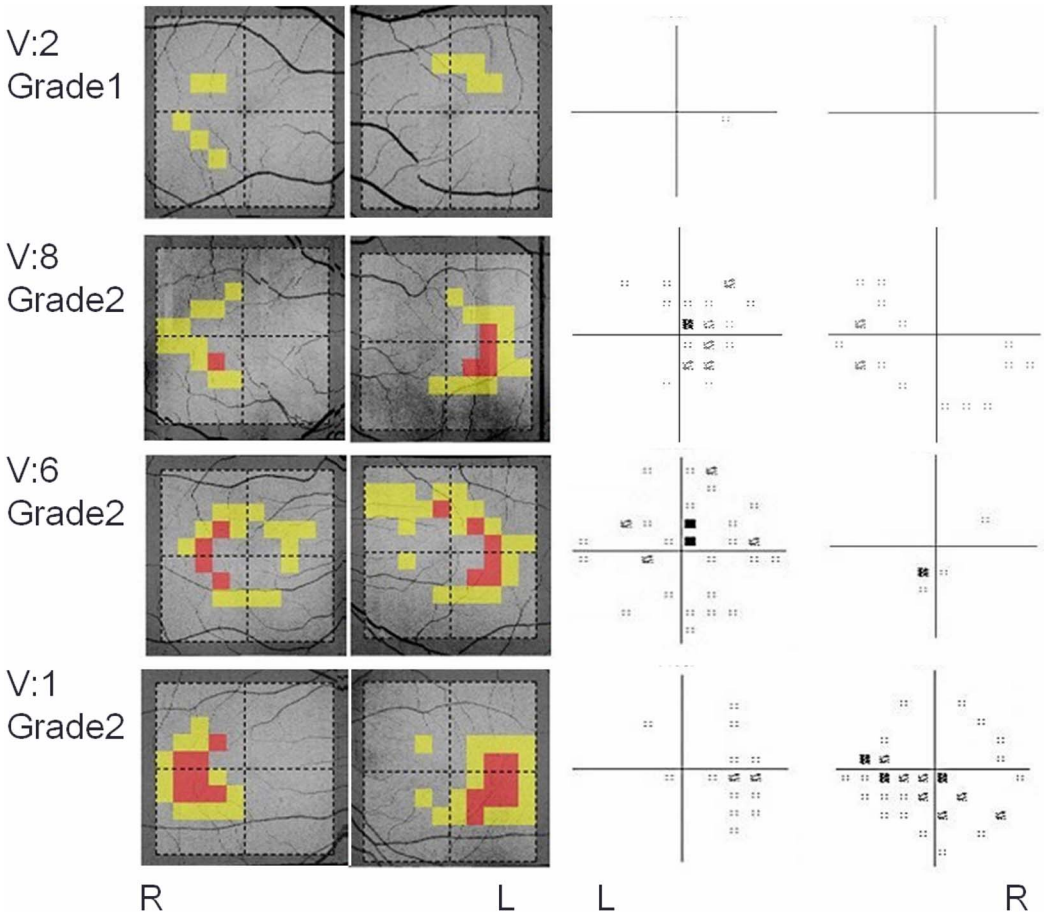

Figure 4. The GCC thickness significance map and the total deviation of the Humphrey visual fields. The GCC thickness significance map obtained from the 3D-OCT 2000 system and the total deviation of the Humphrey visual fields in a patient with grade 2 foveal hypoplasia and autosomal dominant OCA4. Three-dimensional OCT-2000 imaging with a GCC thickness significance map revealed GCC thinning in the temporal region of the fovea of both eyes. The total deviation of the Humphrey visual fields showed a slight reduction of sensitivity in the nasal visual field in a patient with grade 2 foveal hypoplasia.

had typical foveal hypoplasia: 3 had grade 1 (BCVA range, 1.0–1.5), 7 had grade 2 (BCVA range, 0.4–1.5), and 6 had grade 3 (BCVA range, 0.3–0.7) foveal hypoplasia. No patient had grade 4 foveal hypoplasia (Table, Fig. 2). Patients with more severe foveal hypoplasia had poorer visual acuity. In addition, patients with grades 1 and 2 foveal hypoplasia had no or subtle nystagmus, while patients with grade 3 foveal hypoplasia had severe nystagmus.

Pattern VEPs from three patients (V:6, V:8, and V:10) showed a well-defined CI component over the right hemisphere for the left eye, and over the left hemisphere for the right eye. The interhemispheric potential differences for the left and right eyes were opposite in polarity, reflecting the hemispheric asymmetry typically observed in patients with albinism. In a normal member (V:5), the pattern VEP shows no significant interhemispheric asymmetries (Fig. 3).

A macular analysis was performed in 4 patients with grade 1 or 2 foveal hypoplasia using SD-OCT. A GCC thickness significance map revealed GCC thinning at the temporal region of the fovea (Fig. 4). This thinning area was noticeably larger in patients with grade 2 than in those with grade 1 foveal hypoplasia. The 10-2/30-2 Humphrey visual fields showed a very slight reduction of sensitivity in the nasal visual field (Fig. 4).

Iris hypopigmentation was evaluated by a slit-lamp examination. All 16 patients with foveal hypoplasia showed mild hypopigmentation of the irides or hair. Among the 16 patients, 13 had brown hair, which darkened with age, and 3 had black

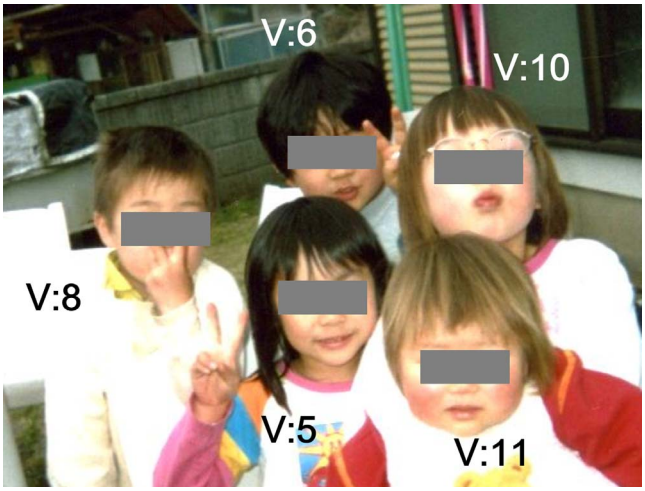

Figure 5. The variable clinical phenotypes of the family members with autosomal dominant OCA4. Patient V:6, with grade 2 foveal hypoplasia, has black hair, which is similar to the unaffected member (V:5). The others (V:8, V:10, and V:11) have light brown hair that darkened with age.

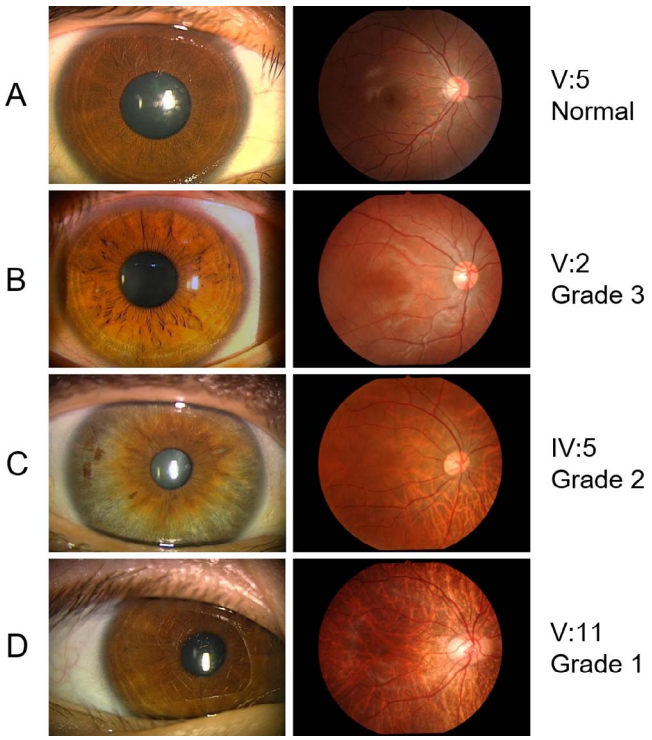

FIGURE 6. The anterior segment and fundus photographs of the patients. The photographs are arranged according to the grades of macular transparency.

hair at presentation (Fig. 5). Three patients had discernible iris hypopigmentation compared to normal Japanese individuals. Ten patients exhibited mild peripheral iris hypopigmentation and 3 had no abnormalities under a slit-lamp examination (Fig. 6). Iris transillumination was not performed, as it is generally undetectable in Japanese patients. Most patients showed skin pigmentation similar to that in normal individuals. Their past histories revealed that their skin was slightly creamy in complexion compared to normal Japanese individuals during the first decade of life. The patients were classified according to their macular transparency grade, as follows: grade 1, $n = 4$ (V:8, IV:6, III:3, V:11); grade 2, $n = 3$ (V:10, IV:3, IV:5); and grade 3, $n = 9$ (IV:4, V:2, IV:1, IV:7, V:1, V:6, III:1, V:9, V:7; Fig. 6).

Parametric linkage analysis with genome-wide SNP markers at a 2 cM interval showed a single candidate region at chromosome 5 (Fig. 7A, upper panel). Further linkage analysis using SNP markers at a 1 cM interval revealed the maximum multipoint parametric LOD score of approximately 3.56 on chromosome 5p13.3-p13.1 with an interval delineated by markers rs13187570 and rs395967 (Fig. 7A, lower panel). The region encompassed 7.2 Mb of length that included the *SLC45A2* gene (See Supplementary Fig.). A novel nonsynonymous sequence change in the coding sequence of the *SLC45A2* gene was found in the proband (V:10):c.208T>C, which predicted a p.Y70H change (Fig. 7B). Codon 70 is located in the second transmembrane domain in the highly conserved MFS/sugar transport protein region spanning codons 35 to 524 (db_xref, CDD: 257676; Fig. 7C). This heterozygous variant was found in all of the affected patients, indicating that the variant cosegregated with the disease. The p.Y70H variant was not found in the Human Gene Mutation Database (available in the public domain at http://www.hgmd.cf.ac.uk), the dbSNP database (available in the public domain at http://www.ncbi.nlm.nih.gov/projects/SNP/), the 1000 Genomes Project (available in the public domain at http://www.1000genomes.org/), or in the NHLBI Exome Sequencing Project (available in the public domain at http://evs.gs.washington.edu/EVS/). We used the Human Genome Variation Database (available in the public domain at http://www.hgvd.genome.med.kyoto-u.ac.jp/), which contains the genetic variations determined by exome sequencing of 1208 Japanese individuals, instead of performing sequencing in human controls; however, the variant was not found. Computational analyses indicated that p.Y70H was "possibly damaging," with a score of 0.950 by PolyPhen-2; "damaging," with a score of 0.013 by SIFT; "deleterious," with a score of −2.93 by PROVEAN; and "disease-causing," with a score of 83 by MutationTaster. The c.208T>C change is considered to be a "likely pathogenic variant with moderate evidence of pathogenicity" according to the latest American College of Medical Genetics (ACMG) standards and guidelines for the interpretation of sequence variants (see Supplementary Table for the pathogenicity based on the ACMG guidelines).[22]

DISCUSSION

Oculocutaneous albinism generally is a group of autosomal recessive disorders which feature hypopigmentation of the hair, skin and eyes.[13] The clinical characteristics of OCA4 are established by the presence of hypopigmentation of the skin and hair, which ranges from complete depigmentation to partial depigmentation with brown hair, and the characteristic ocular changes.[14] We reported a Japanese family in which most members showed foveal hypoplasia and generalized hypopigmentation consistent with OCA4. Mutation screening of the affected members showed a heterozygous missense mutation c.208T>C in the *SLC45A2* gene. To our knowledge, this is the first report to describe autosomal dominant OCA4 in a family in which the diagnosis was confirmed by a mutation analysis. The phenotype was highly variable among subjects with the variant. In general, variable expression is seen more frequently in dominant, rather than recessive, conditions.[23] According to the linkage analysis, a cosegregated gene is less likely to be expected at other regions.

The *SLC45A2* gene is a human orthologue of the mouse underwhite gene (*uw*). Several mutations in the *uw* gene are known to cause melanosome anomalies of varying severity in retinal and coat color.[16] The *uw* series contains a semidominant allele, Uw^{dbr}, which is caused by a p.D153N change. When heterozygous, this change reduces melanin production; when homozygous it results in the loss of nearly all pigmentation.[10] A dominant albino locus also is known in rainbow trout.[15] Contrary, known human mutations in the *SLC45A2* gene are in general believed to be recessive; however, Inagaki et al.[13] suggested that a heterozygous mutation p.D157N can have a dominant-negative effect. The dominant-negative effects occur when a mutated gene product interferes with the function of the normal product (the residual function will be <50%). Dominant-negative mutations often cause recessive phenotypes as exemplified by the mutations in the rhodopsin gene that cause retinitis pigmentosa.[24] A potential diagnosis of the autosomal dominant form of OCA might be overlooked.

Membrane-associated transporter protein, the gene product of *SLC45A2*, is required for normal melanin synthesis, but the molecular mechanism of action remains to be elucidated.[10,21,22] Membrane-associated transporter protein has the highest degree of homology with sucrose/proton symporter proteins, and these transporters in plants and animals have been investigated as the models for MATP.[10,25,26] Notably, mutagenesis studies of plants symporter proteins at a highly conserved residue, located at the end of the first extracellular

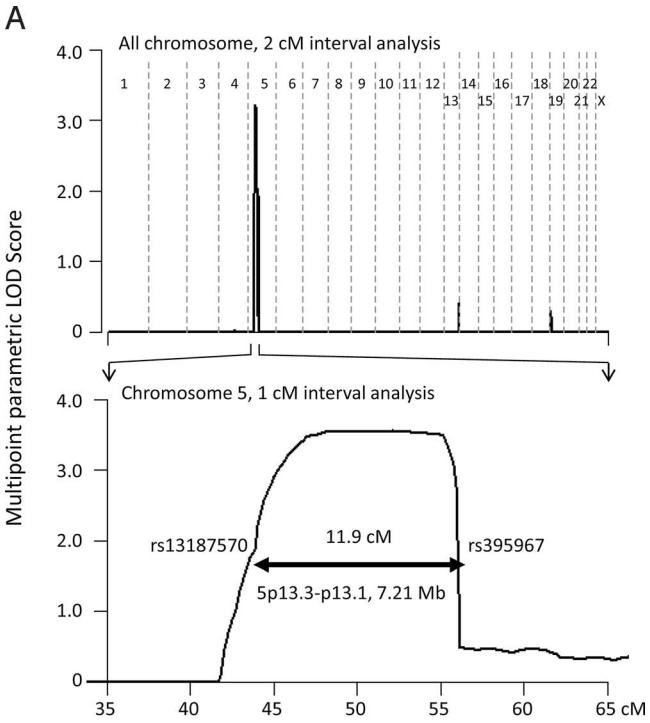

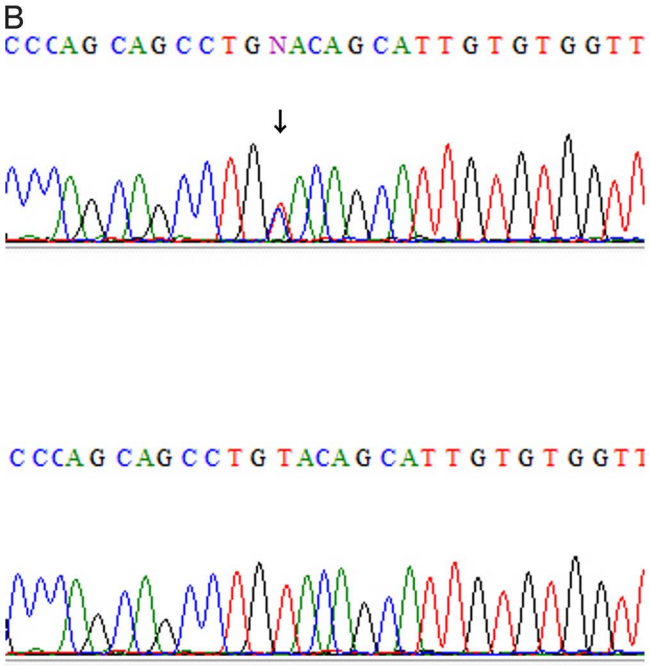

C

	TM1	TM2
	------	-*----------
Human	LLSVGLPSSLYSIVWFLSPIL	
Rhesus:rheMac3	LLSVGLPNSLYSIVWFLSPIL	
Mouse:mm10	LLSVGLPKSLYSMVWLLSPIL	
Elephant:loxAfr3	LLSVGLPKSLYSVVWLLSPIL	
Dog:canFam3	LLSVGLPKSLYSTVWLLSPIL	
X. tropicalis:xenTro7	LLSVGLPRSLYSLVWLISPIL	
Zebrafish:danRer7	LLSVGLPRRLYSLVWLISPIL	
Chicken:galGal4	LLSVGLPKSLYSLVWLISPIL	
Lamprey:petMar2	LLSVGLPRSLYGVVWFISPLL	

loop close to the start of the second transmembrane domain (e.g., H65 of Arabidopsis protein, AtSUC1), have been shown to cause a wide range of abnormal transport activities.[27,28] The diverse activities are attributed to the mutations correlated with the different chemical nature of the residues at this site. These studies imply a functional relevance of the human p.Y70H change since the corresponding codon can be aligned in the immediate vicinity of the H65 codon in AtSUC1 (data not shown). Further functional studies should be performed to determine the extent to which the variant described impairs the function of the protein.

This genetic study has several limitations. Basic research using p.Y70H change is not performed. We did not test an involvement of other 49 genes in the candidate region of the positive LOD score (see Supplementary Figure). However, they were not known to be OCA genes, or to be expressed specifically in the skin and ocular tissues, or function as transport activity according to the UCSC genome browser, available in the public domain at http://genome.ucsc.edu/ .Therefore, the *SLC45A2* gene is highly suggestive for the involvement. We assumed that the high rate of inheritance of the variant occurred by chance, however, unusual families like this are more likely to be studied.

Because the present family with OCA4 exhibited a mild phenotype, it was difficult to distinguish some of the affected members from normally pigmented Japanese individuals. In these subclinical cases, an OCT examination, which sensitively and noninvasively identified foveal hypoplasia, could be helpful for the clinical diagnosis of OCA. The grading of foveal hypoplasia using OCT images was strongly correlated with visual acuity.[16,29] Our patients with low-grade foveal hypoplasia (grade 1 or 2) showed good visual acuity (better than 0.8). Moreover, 9 of 10 patients with low-grade hypoplasia had no nystagmus at the primary position. This finding may represent that the absence of nystagmus is a concomitant feature in patients with albinism with low-grade foveal hypoplasia. Although the mechanisms of reduced acuity in patients with albinism are multifactorial, foveal hypoplasia and nystagmus are the main prognostic indicators for visual acuity, and the severity of both features were well correlated in the present study.

Several members of the family showed strabismus, reduced stereoscopic vision, and interhemispheric asymmetry on VEP recordings, which suggested the misrouting of the optic nerves.[5,30] Many other morphologic anomalies have been reported in the visual pathway of patients with albinism, such as reduced central retinal ganglion cell (RGC) numbers,[31] optic nerves and chiasms of smaller diameter,[32] and decreased lateral geniculate nuclei numbers[33] and gray matter volume at the occipital cortex.[34] These anomalies are likely to be the direct result of decreased ganglion cell numbers in the central retina in albino patients.[33,34] In the present study, the OCT findings showed a significant reduction in the GCC thickness in the

Figure 7. (**A**) Multipoint parametric LOD score in the OCA family. The multipoint parametric LOD scores with a marker interval of 2.0 and 1.0 cM are shown for all chromosomes (*upper*) and for the chromosome 5 candidate region (*lower*), respectively. The 7.2 Mb region between rs13187570 and rs395967 on 5p13.3-p13.1 showed an LOD score of approximately 2.00 to 3.56. (**B**) Sequence trace of the mutation in the *SLC45A2* gene. Sequence traces of the mutation c.208T>C (p.Y70H) in the *SLC45A2* gene in Patient V:10 (*upper*) and unaffected family member V:5 (*lower*). (**C**) The protein sequence alignment of the *SLC45A2* gene with homologues from humans and other vertebrates. These sequences are located in the second transmembrane domain (TM2). *Indicates a corresponding amino acid position that was found in patients with autosomal dominant OCA4.

temporal parafovea in patients with foveal hypoplasia. In general, the development of the foveal pit occurs from 24 weeks of gestation and reaches adult conformation by 15 months postpartum. Changes that occur later in gestation, including the centrifugal migration of the inner retinal layers, result in the progressive reduction of the ganglion and bipolar cell layers at the fovea.[35] Therefore, our GCC significance map data might indicate the incomplete migration of RGCs or the degree of foveal hypoplasia.

Another interesting result in our study is that static perimetry showed a slight reduction of sensitivity in the centronasal visual field. A few studies have assessed visual fields of various forms in human albinism and various findings have been reported, including contracted fields,[36] reduced sensitivity of the central visual field,[37,38] and normal patterns.[39,40] In a previous study which compared the contrast sensitivity of the central, nasal, and temporal retina, some patients with albinism showed the most severe loss in the temporal retina.[36] In contrast, another study demonstrated that the sensitivity of the abnormally projecting part of the temporal retina was not selectively reduced, which indicates that the mechanisms of cortical self-organization result in the abnormal representation available for this visual perception.[41] Another possibility might be the reduction of cone numbers in the central retina due to foveal hypoplasia. This variability of visual function may result from various morphologic and functional anomalies of the visual pathway, including from the retina to the cortex. Further studies are needed to confirm whether the reduced sensitivity of the centronasal visual field is a distinctive finding in human patients with albinism.

The clinical characteristics of a family with foveal hypoplasia and generalized hypopigmentation who were diagnosed with autosomal dominant OCA4 were presented. Most family members exhibited mild general hypopigmentation and low-grade foveal hypoplasia. All of the affected members showed a heterozygous variant, c.208T>C (p.Y70H), in the *SLC45A2* gene, which supported the diagnosis.

Acknowledgments

Disclosure: **R. Oki**, None; **K. Yamada**, None; **S. Nakano**, None; **K. Kimoto**, None; **K. Yamamoto**, None; **H. Kondo**, None; **T. Kubota**, None

References

1. Summers CG, Creel D, Townsend D, King RA. Variable expression of vison in sibs with albinism. *Am J Med Genet*. 1991;40:327–331.
2. Lund RD. Uncrossed visual pathways of hooded and albino rats. *Science*. 1965;149:1506–1507.
3. Creel D, O'Donnell FE Jr, Witkop CJ Jr. Visual system anomalies in human ocular albinos. *Science*. 1978;201:931–933.
4. Guillery RW, Okoro AN, Witkop CJ Jr. Abnormal visual pathways in the brain of a human albino. *Brain Res*. 1975;96:373–377.
5. Creel D, Witkop CJ Jr, King RA. Asymmetric visually evoked potentials in human albinos: evidence for visual system anomalies. *Invest Ophthalmol*. 1974;13:430–440.
6. Apkarian P, Reits D, Spekreijse H. Component specificity in albino VEP asymmetry: maturation of the visual pathway anomaly. *Exp Brain Res*. 1984;53:285–294.
7. Tomita Y, Takeda A, Okinaga S, Tagami H, Shibahara S. Human oculocutaneous albinism caused by single base insertion in the tyrosinase gene. *Biochem Biophys Res Commun*. 1989;164:990–996.
8. Rinchik EM, Bultman SJ, Horsthemke B, et al. A gene for the mouse pink-eyed dilution locus and for human type II oculocutaneous albinism. *Nature*. 1993;361:72–76.
9. Boissy RE, Zhao H, Oetting WS, et al. Mutation in and lack of expression of tyrosinase-related protein-1 (TRP-1) in melanocytes from an individual with brown oculocutaneous albinism: a new subtype of albinism classified as "OCA3." *Am J Hum Genet*. 1996;58:1145–1156.
10. Newton JM, Cohen-Barak O, Hagiwara N, et al. Mutations in the human orthologue of the mouse underwhite gene (*uw*) underlie a new form of oculocutaneous albinism, OCA4. *Am J Hum Genet*. 2001;69:981–988.
11. Montoliu L, Gronskov K, Wei A-H, et al. Increasing the complexity: new genes and new types of albinism. *Pigment Cell Melanoma Res*. 2013;27:11–18.
12. Suzuki T, Tomita Y. Recent advances in genetic analyses of oculocutaneous albinism types 2 and 4. J *Dermatol Sci*. 2008;51:1–9.
13. Inagaki K, Suzuki T, Shimizu H, et al. Oculocutaneous albinism type 4 is one of the most common types of albinism in Japan. *Am J Hum Genet*. 2004;74:466–471.
14. Inagaki K, Suzuki T, Ito S, et al. Oculocutaneous albinism type 4: six novel mutations in the membrane-associated transporter protein gene and their phenotypes. *Pigment Cell Res*. 2006;19:451–453.
15. Nakamura K, Ozaki A, Akutsu T, et al. Genetic mapping of the dominant albino locus in rainbow trout (*Oncorhynchus mykiss*). *Mol Genet Genomics*. 2001;265:687–693.
16. Sweet HO, Brilliant MH, Cook SA, Johnson KR, Davisson MT. A new allelic series for the underwhite gene on mouse chromosome 15. *J Hered*. 1998;89:546–551.
17. Summers CG, Knobloch WH, Witkop CJ Jr, King RA. Hermansky-Pudlak syndrome: ophthalmic findings. *Ophthalmology*. 1988;95:545–554.
18. Thomas MG, Kumar A, Mohammad S, et al. Structural grading of foveal hypoplasia using spectral-domain optical coherence tomography. A predictor of visual acuity? *Ophthalmology*. 2011;118:1653–1660.
19. Kruglyak L, Daly MJ, Reeve-Daly MP, Lander ES. Parametric and nonparametric linkage analysis: a unified multipoint approach. *Am J Hum Genet*. 1996;58:1347–1363.
20. Hoffmann K, Lindner TH. easyLINKAGE Plus—automated linkage analyses using large-scale SNP data. *Bioinformatics*. 2005;21:3565–3567.
21. Broman KW, Murray JC, Sheffield VC, White RL, Weber JL. Comprehensive human genetic maps: individual and sex-specific variation in recombination. *Am J Hum Genet*. 1998;63:861–869.
22. Richards S, Aziz N, Bale S, et al. Standards and guidelines for the interpretation of sequence variants: a joint consensus recommendation of the American College of Medical Genetics and Genomics and the Association for Molecular Pathology. *Genet Med*. 2015;17:405–424.
23. Strachan T, Read A. *Genes in Pedigrees and Populations*. *Human Molecular Genetics*. 4th ed. New York: Tayler & Francis Group; 2011:61–90.
24. Rajan RS, Kopito RR. Suppresion of wild-type rhodopsin maturation by mutants linked to autosomal dominant retinitis pigmentosa. *J Biol Chem*. 2005;280:1284–1291.
25. Reinders A, Ward JM. Investigating polymorphisms in membrane-associated transporter protein SLC45A2, using sucrose transporters as a model. *Mol Med Rep*. 2015;12:1393–1398.
26. Meyer H, Vitavska O, Wieczorek H. Identification of an animal sucrose transporter. *J Cell Sci*. 2011;124:1984–1991.
27. Lemoine R. Sucrose transporters in plants: update on function and structure. *Biochim Biophys Acta*. 2000;1465:246–262.

28. Lu JM, Bush DR. His-65 in the proton-sucrose symporter is an essential amino acid whose modification with site-directed mutagenesis increases transport activity. *Proc Natl Acad Sci U S A*. 1998;95:9025–9030.
29. Seo JH, Yu YS, Kim JH, Choung HK, Heo JW, Kim SJ. Correlation of visual acuity with foveal hypoplasia grading by optical coherence tomography in albinism. *Ophthalmology*. 2007;114:1547–1551.
30. Lee KA, King RA, Summers CG. Stereopsis in patients with albinism: clinical correlates. *J AAPOS*. 2001;5:98–104.
31. Jeffery G, Kinsella B. Translaminar deficits in the retinae of albinos. *J Comp Neurol*. 1992;326:637–644.
32. Schmitz B, Schaefer T, Krick CM, Reith W, Backens M, Kasmann-Kellner B. Configuration of the optic chiasm in humans with albinism as revealed by magnetic resonance imaging. *Invest Ophthalmol Vis Sci*. 2003;44:16–21.
33. Mcketton L, Kelly KR, Schneider KA. Abnormal lateral geniculate nucleus and optic chiasm in human albinism. *J Comp Neurol*. 2014;522:2680–2687.
34. von dem Hagen EA, Houston GC, Hoffmann MB, Jeffery G, Morland AB. Retinal abnormalities in human albinism translate into a reduction of grey matter in the occipital cortex. *Eur J Neurosci*. 2005;22:2475–2480.
35. Hendrickson AE, Yuodelis C. The morphological development of the human fovea. *Ophthalmology*. 1984;91:603–612.
36. St John R, Timney B. Sensitivity deficits consistent with aberrant crossed visual pathways in human albinos. *Invest Ophthalmol Vis Sci*. 1981;21:873–877.
37. Edmunds RT. Vision of albinos. *Arch Ophthalmol*. 1949;42:755–767.
38. Abadi RV, Pascal E. Incremental light detection thresholds across the central visual field of human albinos. *Invest Ophthalmol Vis Sci*. 1993;34:1683–1690.
39. Marmor MF, Choi SS, Zawadzki RJ, Werner JS. Visual insignificance of the foveal pit: reassessment of foveal hypoplasia as fovea plana. *Arch Ophthalmol*. 2008;126:907–913.
40. Kubal A, Dagnelie G, Goldberg M. Ocular albinism with absent foveal pits but without nystagmus, photophobia, or severely reduced vision. *J AAPOS*. 2009;13:610–612.
41. Hoffmann MB, Seufert PS, Schmidtborn LC. Perceptual relevance of abnormal visual field representations: static visual field perimetry in human albinism. *Br J Ophthalmol*. 2007;91:509–513.

Investigative Ophthalmology & Visual Science